ELSEVIER

Journal of Chromatography A, 791 (1997) 135–149

JOURNAL OF CHROMATOGRAPHY A

Effects of flow-rates and sample concentration on the molar mass characterisation of modified celluloses using asymmetrical flow field-flow fractionation–multi-angle light scattering

Bengt Wittgren*, Karl-Gustav Wahlund

Division of Technical Analytical Chemistry, Center for Chemistry and Chemical Engineering, Lund University, P.O. Box 124, S-221 00 Lund, Sweden

Received 25 April 1997; received in revised form 4 July 1997; accepted 31 July 1997

Abstract

Modified celluloses are an important group of polymers used in many applications, such as in the food and drug industry. Thus, their physicochemical properties are of considerable interest and need to be characterised carefully. In this study, asymmetrical flow field-flow fractionation (asymmetrical flow FFF) connected on-line to a multi-angle light scattering (MALS) detector was used to study the molar mass and molar mass distribution of three different hydroxypropylmethylcelluloses (HPMCs). The influence of the flow-rates and the sample concentration on the results obtained was found to be significant, emphasising the importance of optimising the experimental conditions so as to obtain reliable information about the polymer system. With the use of appropriate conditions, flow FFF–MALS was found to be a suitable method for the characterisation of these complex samples. The weight-average molar mass ranged from 132 000 g/mol to 309 000 g/mol. The *z*-average radius of gyration was found to be high relative to the molar mass, ranging from 58 nm to 73 nm, suggesting an expanded structure. This was also confirmed by double logarithmic plots of the molar mass versus the radius of gyration, the slope being approximately 0.7 for the two high molar mass samples.

Keywords: Field-flow fractionation; Molar mass characterisation; Asymmetrical flow field-flow fractionation; Multi-angle light scattering; Cellulose, modified

1. Introduction

Hydroxypropylmethylcellulose (HPMC) belongs to a group of polysaccharides well-known in the food and pharmaceutical industry [1–3]. Among other applications, they are used as excipients in drug formulations. Thus, there is an obvious need of information regarding their physicochemical properties. However, modified celluloses are difficult to characterise due to their frequent high polydispersity and complex solution behaviour [2]. Two of the most important features to determine are their molar mass and mass distribution. Determination of these properties is usually not straightforward, as exemplified in recent studies [2,3]. In one of these, it was found that a set of different techniques was often needed to provide an adequate picture of such complex samples [2]. One technique that can be regarded as a useful alternative to techniques traditionally used is flow field-flow fractionation (flow FFF), a method of separation particularly well suited for the fractionation and characterisation of large macromolecules

*Corresponding author.

0021-9673/97/$17.00
PII S0021-9673(97)00831-5

and particles of varying origin. The method is universal and can deal with a very wide size range of the sample, from 1 nm up to 50 μm [4,5], of major advantage in characterising large and polydisperse polysaccharides.

Connecting flow FFF to a multi-angle light scattering detector (MALS), greatly increases the applicability of the method to polymers. Using this hyphenation, it is possible to obtain absolute molar mass and distributions directly [6,7]. A previous study demonstrated the power of this combination of methods in the characterisation of various model polysaccharides [8]. In that study, flow FFF–MALS was found to be very fast and efficient in obtaining molar mass, as well as information on the radius of gyration and on conformation. That work is continued here, being applied to the more complex HPMC polymers. Special attention is directed at the effects of different sample concentrations and flow-rates on the fractionation of three HPMC samples that are examined. The aim is to provide guidelines concerning use of flow FFF so as to optimise the molar mass fractionation of complex polymers and obtain realistic distributions. The data obtained are compared with results obtained using osmometry.

2. Theory

Flow FFF is a separation method applicable to macromolecules, colloids and particles in the sub-micron and micron size range [4]. Like other FFF-techniques, it utilises thin, flat channels along which a carrier liquid is continuously pumped. The injected sample is transported axially along the channel by this flow. The size fractionation is initiated by a force acting perpendicular to the channel flow. This force consists of a secondary flow, the so-called crossflow, which compels the sample components to move towards one of the channel walls, the accumulation wall, usually consisting of an ultrafiltration membrane permeable to the flow. This movement, in turn, is counteracted by size-dependent diffusion which results in the fact that differently sized sample components differ in the position above the accumulation wall. Due to the parabolic velocity profile of the channel flow, differently positioned components are transported at differing speed. Consequently, there is a separation in time due to differences in diffusion coefficients, i.e., to hydrodynamic size.

The principle of asymmetrical flow FFF is shown in Fig. 1 [9–11]. In the version of flow FFF

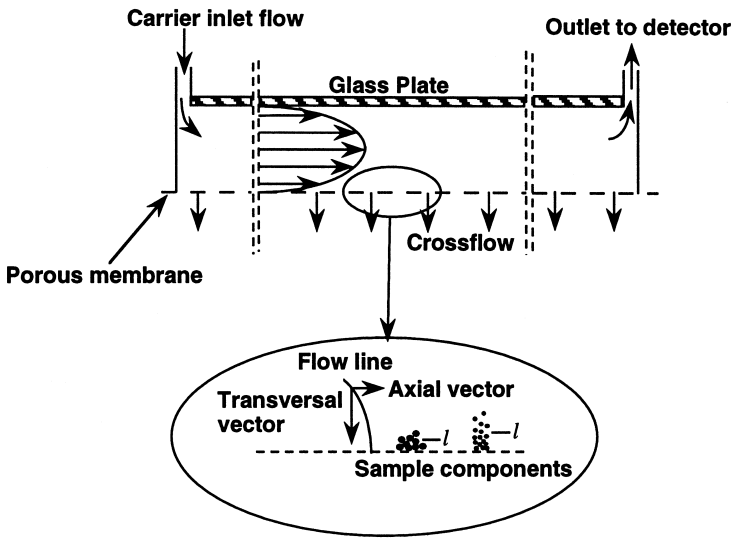

Fig. 1. Schematic presentation of the principle of asymmetrical flow FFF. The carrier inlet flow is directed either towards the channel outlet or through the porous membrane. Thus, the sample components are subjected both by an axial flow vector, which transports them towards the outlet and towards the detector (outlet flow), and by a transversal flow vector that presses them towards the membrane (crossflow). The transport time along the channel is dependent on the position, l of the centre of mass above the membrane, which in turn is determined by the diffusion coefficient of each component.

employed here, one wall is permeable to the liquid [9], whereas the other wall is solid, consisting of a glass plate. Accordingly, the crossflow, which in symmetrical flow FFF is pumped independently through the entire cross section of the channel, is generated here from the part of the channel flow that exits through the membrane. The inlet flow-rate V_{in} is thus divided into the outlet flow-rate V_{out} and the crossflow-rate V_c

$$V_{in} = V_c + V_{out} \quad (1)$$

The level of retention, defined as the ratio of the retention time t_r to the void time t^0, of a species having the diffusion coefficient D depends directly on V_c according to

$$\frac{t_r}{t^0} \approx \frac{w^2 V_c}{6DV^0} \quad (2)$$

where V^0 and w are the volume and the thickness of the separation channel, respectively [5,9,10]. For $t_r/t^0 \geq 2.3$, the error in Eq. (2) is less then 10% [5]. t^0 is calculated from experimental parameters and decreases when V_c increases [10]. A higher level of retention, and thus increased resolution [11], can therefore be achieved by an increase in V_c.

Obviously, the flow FFF instrument has the ability to fractionate macromolecules that differ in size and shape. This ability is taken advantage of by the combination of flow FFF with a multi-angle light scattering instrument. This makes it possible to obtain the Rayleigh ratio R_θ in each small slice i of the fractionated sample [6] according to

$$\frac{Kc_i}{R_{\theta i}} = \frac{1}{P(\theta)M_i} + 2A_2 c \quad (3)$$

where c is the sample concentration, A_2 is the second virial coefficient, M is the molar mass, θ is the scattering angle and K an instrumental constant. The form factor $P(\theta)$, which is connected to the radius of gyration r_G, is usually given in its reciprocal form

$$P(\theta)_i^{-1} = 1 + \frac{16\pi^2\langle r_G^2\rangle_i}{3\lambda^2}\sin^2\left(\frac{\theta}{2}\right) \quad (4)$$

where λ is the wavelength of the light.

The concentration of the polymer in each slice is determined simultaneously by an inline concentration detector, such as a refractive index detector or a UV detector. This allows both distributions and averages to be obtained for both the molar mass and the radius of gyration [6]. Consequently, the polydispersity index, M_w/M_n, an important parameter in polymer characterisation, can also be obtained available from flow FFF–MALS measurements.

3. Experimental

3.1. Materials

Three HPMC 2910 samples of differing viscosity grades were analysed: HPMC 2910 10000 cps (''HPMC 10000'') (Methocel E10M, Dow Chemicals, Midland, USA), HPMC 2910 4000 cps (''HPMC 4000'') (Methocel E4M, Dow Chemicals) and HPMC 2910 50 cps (''HPMC 50'') (Metolose 60SH-50, Shin-Etsu, Japan). The number average molar masses for these sample, as determined by osmometry [12], are seen in Table 1. The solid material (water content 3%) was dispersed in a hot

Table 1
The weight average molar mass, M_w, the number average molar mass, M_n, the z-average radius of gyration r_{Gz} and the polydispersity index, M_w/M_n obtained from FFF–MALS show the difference in size and polydispersity between the HPMC samples

Sample	Parameter					
	M_w (g/mol)	M_n (g/mol)	M_n^1 (g/mol)	r_{Gz} (nm)	M_w/M_n	Recovery (%)
HPMC 10000	309 000	158 000	120 000	73	2.0	93
HPMC 4000	225 000	117 000	100 000	68	1.9	86
HPMC 50	132 000	35 000	31 000	58	3.7	88

M_n-values obtained from osmometry are included as comparison. The recovery of each sample injected is obtained from the refractometer.
[1] Obtained by osmometry [12].

carrier liquid at 65°C that was cooled in a refrigerator overnight so as to dissolve the polymer. The carrier liquid was a filtered mixture of 50% (v/v) methanol (HPLC-grade, Merck, Darmstadt, Germany) and 0.010 *M* sodium chloride (analytical-reagent grade, Merck). The filter employed was a 0.2 μm regenerated cellulose filter SM 116 (Sartorius, Göttingen, Germany). The temperature in the carrier was approximately 24°C.

3.2. Methods

The complete FFF–MALS setup is shown in Fig. 2. The separator was an ordinary asymmetrical flow FFF instrument described earlier [5,11]. The separation channel had a trapezoidal geometry defined by a Mylar (polymethylmetacrylate) spacer. The channel length L was 28.6 cm and the breadths of the channel, b_0 and b_L were 2.1 cm and 0.54 cm, respectively. The accumulation wall had an area of 33.65 cm^2. The channel thickness was calibrated by ferritin [11] to 0.0119 cm, yielding a channel volume of 0.400 cm^3. The accumulation wall consisted of an ultrafiltration membrane of regenerated cellulose, NADIR UF-10c, cutoff 10 000 g/mol (Hoechst, Wiesbaden, Germany). Two Kontron HPLC pumps 420 (M-head; max flow-rate 10 ml/min) (Kontron Instruments, Zurich, Switzerland) were employed for delivering the carrier flow (pump 1) and injection flow (pump 2), respectively. The motor driven valves V1 and V2 directed the flow in each fractionation according to the current experimental phase [5]. V1 was a Valco E-CST 4UV multi-position valve and V2 a Valco E C4W 2 position valve (Vici, Valco Europe, Schenkon, Switzerland). The sample was injected by a Rheodyne 9125 syringe injector (Rheodyne, Cotati, CA, USA) with a 20-μl sample loop. The outlet flow-rate was monitored online by a PhaseSep liquid flow meter (Phase Separations, Queensferry, UK). Three fine metering needle valves (Hoke Valve 1656 G2YA, Hoke, Cresskill, NJ, USA) were employed. Two of them, N1 and N2 in Fig. 2, were employed to regulate the flow-rates V_{out} and V_c, respectively, and the third to regulate the flow directions at the relaxation/focusing phase [5]. The flow-rate during this phase was 1.5 ml/min. The flow-rates delivered by pump 1 and the motor-valves V1 and V2 were directed by a Kontron Data System 450-MT2 (Kontron Instruments, Zurich, Switzerland). For a more precise description of the operational procedures of the asymmetrical flow FFF system, the reader is referred to earlier publications [5,11]. A stainless-steel high-pressure filter holder, 25 mm, (Millipore, Bedford, MA, USA), F1, with a 25 mm 0.1 μm filter (Anodisc 25, Anotec Separations, Banbury, UK) was connected directly to pump 1 on-line. F2 was a small volume pre-column filter A315 (Upchurch Scientific, Oak Harbor, WA, USA) with a replaceable stainless-steel frit A 101x (pore size 2 μm) employed in-line between the channel and the detector as described earlier [8]. The frit served as support for a regenerated cellulose filter paper (SM 116 Sartorius) the pore size of which was 0.45 μm. It cannot be excluded that such a filter

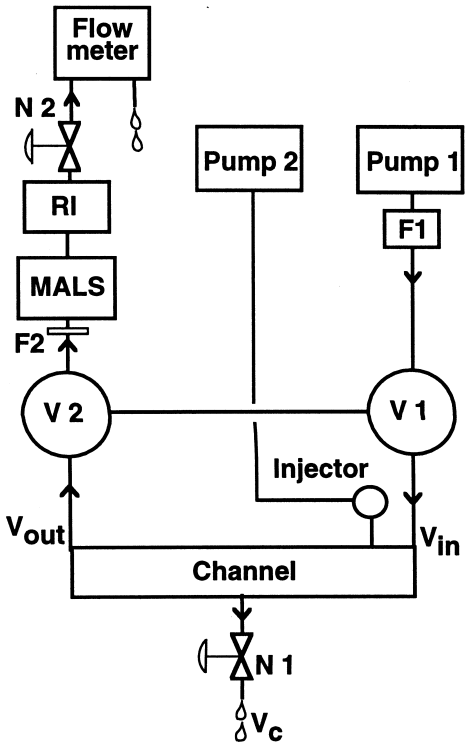

Fig. 2. Simplified presentation of the combined asymmetrical flow FFF–MALS system showing the elution phase. The two detectors, MALS and RI, are connected to the channel outlet via the inline filter F2 (pore size 0.45 μm). The carrier flow from pump 1 is purified by the inline filter F1 having a pore size of 0.02 μm. The crossflow-rate versus the outlet flow-rate is adjusted by needle valves, N1 and N2, the outlet flow-rate being measured continuously by a flow meter.

would influence the results by removing sample material. Therefore, it is important that results, with and without the filter F2 are compared for every different experimental condition. This was done in this study and it was found that the filter F2 greatly decreased the noise of the baseline without causing any detectable losses of the sample.

The light scattering photometer was a DAWN-DSP multi-angle light scattering instrument (Wyatt Technology, Santa Barbara, CA, USA). Simultaneous concentration detection was performed using an Optilab DSP interferometric refractometer (Wyatt). Both detectors used a wavelength of 633 nm. Filtered toluene (Merck) was used for calibration of the MALS-detector and sodium chloride (Suprapur, Merck) for calibration of the refractive index detector. The detectors at different angles in the MALS instrument were normalised to the 90° detector using low polydisperse pullulan P-50 (Shodex STANDARD P-82, Showa Denko, Tokyo, Japan) and bovine serum albumin (BSA) (Sigma, St. Louis, MO, USA) at a flow-rate through the detectors of 1 ml/min. BSA was also used to determine the interconnection volume between the detectors to 0.137 ml. The flow-rate through the detectors, V_{out}, was constantly held at about 1 ml/min. Since it was in principle unchanged from run-to-run, it did not require any renormalisation of the MALS instrument. The signals from the two detectors were analysed by ASTRA software (ASTRA for Windows 4.2) (Wyatt Technology). The recovery was obtained from the ratio of the mass eluted from the channel (determined by integration of the refractometer signal) to the mass injected [8]. The molar mass and radius of gyration values were obtained from linear plots of $Kc_i/R_{\theta i}$ against $\sin^2(\theta/2)$ according to Eqs. (3) and (4). In these plots, scattering intensities from at least 10 different angles were employed.

The (dn/dc) parameter was determined by the injection of six different concentrations of each of the HPMC samples into the refractometer. During these measurements, the injector, equipped with a 1.0 ml loop, was connected to the refractometer directly. The flow-rate employed was 0.6 ml/min which was found to be sufficient for obtaining good and consistent data. The data were analysed using the DNDC5 software (Wyatt Technology). The (dn/dc) values obtained were 0.119, 0.120 and 0.132 for HPMC 10000, HPMC 4000 and HPMC 50, respectively.

4. Results and discussion

Previous work indicated many potential advantages of flow FFF in the separation of polymers [5,8,13–18], specifically those of its being applicable to large macromolecules since no upper limit are placed on molar mass, to the broad distributions and broad range of molar mass that can be dealt with, to the rapidity of separations so that analysis times of only a few minutes are required [8], and to the possibility of determining diffusion coefficients without any calibration procedure being needed. These advantages have been tested in various applications [7,8,16,17] mainly on certain standard polymers and particles and found to be representative.

A MALS detector provides a comfortable way of obtaining the absolute molar mass and, by combining it with a separation technique, of obtaining distributions as well. Care must be taken, however, to optimise the experimental conditions in order to ensure optimum fractionation, since otherwise the accuracy of the molar mass distribution and the average molar masses obtained can be affected. In flow FFF, separation occurs on the basis of differences in the diffusion coefficients. Measurements of molar mass distributions thus require that the diffusion coefficients depend in a consistent way on the molar mass, decreasing as molar mass increases. Thus, the fractogram obtained needs to represent a consistent ordering of the fractionation of molar masses over the elution times observed. With increasing resolution of the molar masses, the accuracy of the molar mass distribution obtained increases. Thus, it is just as important as without any MALS detector to focus on the performance of the separation technique and investigate how various experimental parameters influence the separation.

In the case of flow FFF, it is important that the effects of variations in flow-rates are studied so that good resolution can be obtained [11]. Too mild retention, low t_r/t^0 ratio, can result in poor fractionation of the molar masses involved, due to a lowering of both the separation selectivity [19] and

efficiency [11,20] yielding an underestimation of polydispersity.

The concentration of the sample also plays an important role. A high sample load is required for samples of low molar mass so as to increase the signal-to-noise ratio on the MALS detector, which may otherwise be too low. A disadvantage of a high sample load is that of overloading effects [21] and thus reduced resolution.

The amphiphilic nature of HPMC-polymers makes them sensitive to the composition of the solvent. For example, a mixture of 50% methanol and 50% 10 m*M* aqueous NaCl has been found to provide a more suitable hydrophilic/hydrophobic balance in solubility than pure water does [2]. Consequently, the influence of different solvents on solution behaviour is another effect of fundamental importance that needs characterisation.

The present study considers the effects of flow-rate and sample concentration on the obtained molar mass of three HPMC samples of differing size. The solvent consisted of a mixture of 50% methanol and 50% 10 m*M* aqueous NaCl. The crossflow-rate V_c was varied from 0.25 ml/min to 2.0 ml/min and the concentration of the samples from 1 mg/ml to 12 mg/ml. The results of these variations are demonstrated and the obtained molar mass and radius of gyration for these samples are discussed.

4.1. Flow-rate effects

In flow FFF, the crossflow-rate V_c determines the retention level according to Eq. (2) [5]. In working with flow FFF–MALS, V_c is normally increased by applying a higher inlet flow-rate V_{in} at constant V_{out}, i.e., by increasing the V_c/V_{out} ratio. A suitable retention level in flow FFF is usually considered to be in the range of $6<t_r/t^0<40$ [5,21]. For globular proteins and spherical particles, which have comparably high diffusion coefficients due to their compact shape, V_c must be relatively high for a sufficient retention level to be achieved. For example, ferritin, a globular protein with a molar mass of 440 000 g/mol, higher than that of HPMC 10000, requires a crossflow-rate of 5–7 ml/min (V_c/V_{out}, ratio of 5–10) for a retention level of 10–15 to be attained. Working with flexible polymers similar to these in their range of molar mass, the more expanded conformation results in a lower diffusion coefficient, which requires a lower crossflow-rate.

Another important factor is the low overlap concentration of expanded polymers. The sample zone concentration becomes greater when the crossflow-rate increases [10,11], which with macromolecules such as these can cause entanglement and changes in viscosity. At a high crossflow, the distance to the ultrafiltration membrane is also short, increasing the possibilities for sample–membrane interactions. The effect may be a change in the elution behaviour of the sample, resulting in too short (repulsion) or too long (adsorption) a retention time. On the other hand, too small a crossflow can result in poor fractionation of the molar masses and thus in misleading molar mass distributions being obtained. The choice of good flow conditions is also difficult in working with polydisperse polymers. There are thus good reasons to investigate carefully the influence of flow conditions on the results obtained. This should be regarded as a standard procedure in the molar mass characterisation of polymers.

The number average molar mass of the HPMC samples has been determined by osmometry [12] the results obtained being shown in Table 1. Osmometry provides no information, however, on the polydispersity or size of these polymers. Since HPMC polymers can serve as viscosity regulators, they were considered to be quite expanded. Accordingly, initial experiments were carried out at a low V_c/V_{out} ratio. The experiments began at the very low V_c of 0.25 ml/min. This was then increased in four steps up to 2 ml/min. The mass of each of the three HPMCs injected was about 100 μg. The fractograms for HPMC 10000 obtained at different V_c are shown in Fig. 3. At the lowest V_c (Fig. 3A), the t_r/t^0 ratio is likewise very low, only about 2 at the RI peak maximum, the peaks not being resolved from the disturbing void peaks. Such a void peak can be caused by material having such low molar mass so that it is not retained. Other possibilities are that it contains material (of various molar masses) that has not been completely relaxed to its equilibrium distance from the ultrafilter, or that it contains very large aggregates (>500 nm) migrating in the hyperlayer mode. The latter does not appear possible in this case, however, since inline filter F2 should have removed such aggregates.

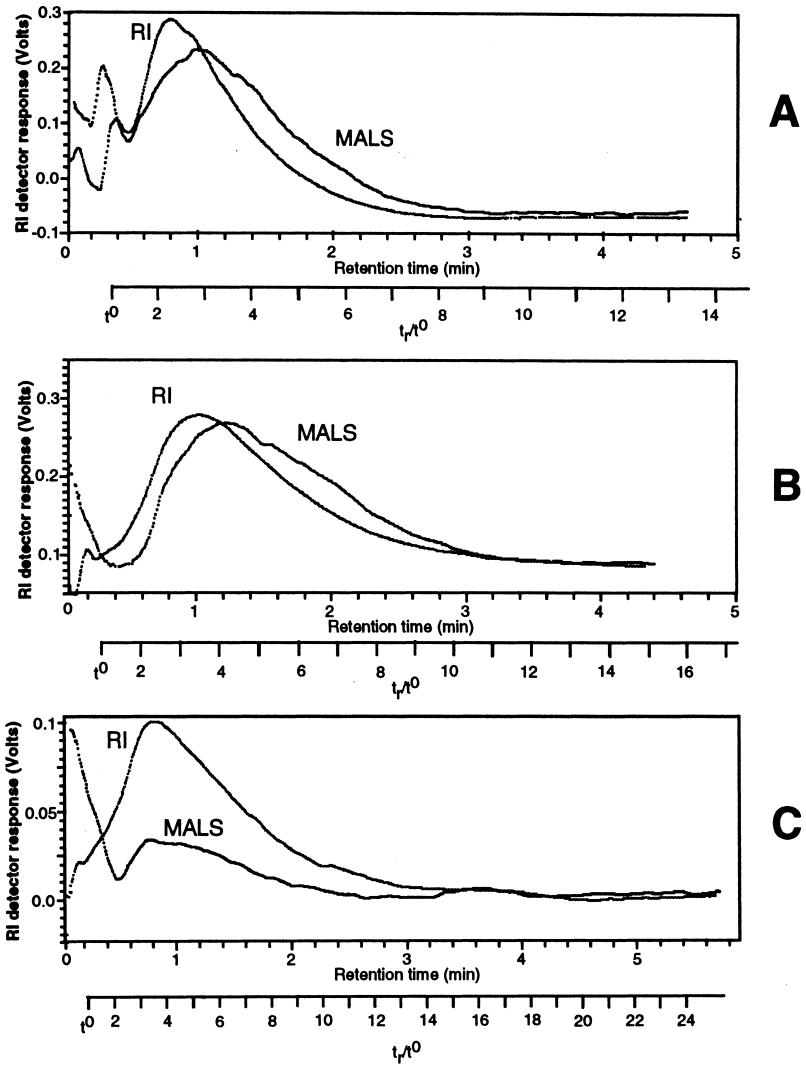

Fig. 3. Combined MALS and RI fractograms for HPMC 10000 at different inlet flow-rates and constant outlet flow-rates. The MALS fractogram is obtained from the 90° detector. The RI detector response can be read off at the *y*-axis. The MALS detector response is plotted directly proportional to the RI signal in the fractograms. Conditions: (A) $V_{in}=1.25$ ml/min; $V_c=0.25$ ml/min; $V_c/V_{out}=0.25$; $t^0=0.35$ min; (B) $V_{in}=1.75$ ml/min; $V_c=0.75$ ml/min; $V_c/V_{out}=0.75$; $t^0=0.29$ min and (C) $V_{in}=3.0$ ml/min; $V_c=2.0$ ml/min; $V_c/V_{out}=2$; $t^0=0.22$ min. The sample concentration was 5.14 mg/ml.

In order to increase the retention level, the inlet flow-rate was increased. At $V_c=0.75$ ml/min, Fig. 3B, the resolution between the peaks and the void time was much enhanced, the detector signals reaching the baseline before elution of the sample material had begun. The void peak observed in Fig. 3A had in this case disappeared, indicating the latter to not have been caused by low molar mass components. The unstable and drifting detector signals remaining, which occur between the start of elution and the void time, are caused by flow instabilities in the detector cells during the period following the onset of flow when switching from the relaxation/focusing phase to the elution phase takes place [5,11]. These signals do not disturb the analysis under such conditions. Drifting signals of this sort may sometimes reach

beyond the void time period, as shown in Fig. 3A Fig. 3C, resulting in the detector signals being disturbed and the perturbing of information concerning the low molar mass part of the sample. It is highly desirable, therefore, to have a baseline separation between the peak and the void time.

A further increase in V_c to 2.0 ml/min (Fig. 3C) caused a dramatic decrease in the refractometer signal, especially the MALS signal, the obtained recovery being only around 50%. The peak profiles shown in Fig. 3C appear not to be more retained than in Fig. 3B despite a higher crossflow-rate being applied. It is possible that the non-eluted fraction of the sample consists of larger material that would normally have led to higher responses at the high retention level end of the peak profile. The explanation of the elution of such components being disturbed may be that the higher crossflow, which presses the polymer chains closer to the membrane and leads to higher concentrations, causes entanglement. Since the retention level of the interacting components then will be very high, it is possible that they are eluted so slowly that they never leave the channel at all during the elution phase. Thus, the upper limit in retention level at which sample components are lost or sample zones are excessively broadened is much lower for expanded polymers than for compact spheres and globular proteins [21]. This calls for carefully performed experiments.

According to Eq. (3), the molar mass is obtained directly from the detector responses for each slice in the fractionated peak. This is shown in Fig. 4, in which the experiments depicted in Fig. 3 are involved, the molar mass versus the elution time being plotted for HPMC 10000 at the three different crossflow-rates. The optimum experimental conditions in Fig. 4 should be those yielding curve B due to the fractogram shown in Fig. 3B appears least disturbed by detector drift or void peaks. The signals collected down to as low as 0.5 min, where the MALS signal reaches the baseline, can be employed. The molar mass curve thus increased steadily over time within a broad range of molar mass, from 100 000 g/mol up to 900 000 g/mol. The initial part of the curve has a much steeper slope. Although this might be explainable in terms of a decrease in the mass selectivity, dln t_r/dln M, of FFF, the onset of such an effect would be expected to occur at a very

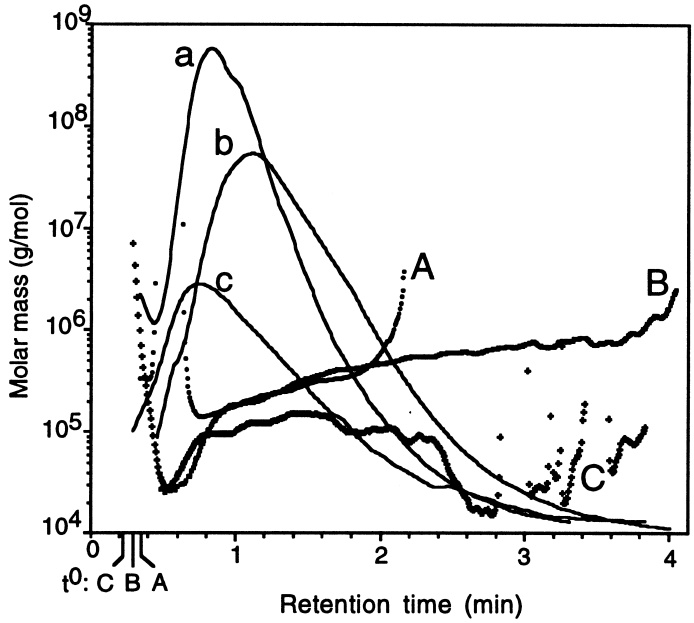

Fig. 4. Molar mass versus elution time for HPMC 10000 at different flow-rates. The refractometer signal is superimposed. The capital letters correspond to the molar mass curves and the lower case letters to the refractometer signal of each fractogram. Conditions were identical to Fig. 3, the lettering A, B, C corresponding directly to Fig. 3A,B,C, respectively.

much lower retention level than the t_r/t^0 ratio of between 2 and 3 observed in Fig. 4. Therefore, an experimental disturbance, e.g., a difference in the band broadening between the two detectors [7], seems probable.

For the lowest V_c (curve A), there is a reasonable increase in molar mass over time except at the high and low ends of the molar mass scale where the molar mass appears to be markedly overestimated. At the high end of the scale, this might possibly be explained by a sudden decrease in mass selectivity in the separation but it is hard to find a reason for this. Another theoretical possibility is that the polymer aggregates to form very compact structures, but this would have produced a stronger signal on the MALS detector. A more reasonable explanation would be that the excess in molar masses observed is due to an error in the close to baseline RI detector signal based on the low concentration at the high molar mass end. Similar effects have been reported in other applications using flow FFF–MALS [7,8]. At the low molar mass end, the overestimation of the molar mass is most probably a disturbance caused by the presence of the void peak and the drift in the detector signals in the vicinity of the void time, as can be seen in Fig. 3A.

The increase in V_c to 2 ml/min (curve C) resulted in a reasonable increase in molar mass over time, from 80 000 g/mol to only 130 000 g/mol. The improvement in measurement of the low molar masses is due to these components having shifted to higher retention levels, i.e., being better resolved from the void time. The overestimation of molar masses below 0.5 min is artifactual as was discussed in connection with curve A. At higher retention (>2 min), the high noise of the weak MALS signal leads to the molar mass values obtained being highly fluctuating and unreliable. Useful data can only be collected, therefore, during the rather short interval of 0.8 to 1.8 min. However, this covers a large mass fraction of the eluted concentration profile (curve C).

From Eq. (2) it is obvious that a given molar mass, corresponding to a particular diffusion coefficient, only is present at the same retention time if all the other parameters are constant. The fact that curves A and B coincide for elution times of between 1 and 2 min thus reflects, in fact, an experimental error, since both V_c and t^0 were different in these two experiments. A better presentation of the molar mass data in Fig. 4 can be obtained if the well known relationship between the diffusion coefficient and the molar mass, $D=AM^{-b}$ (where b depends on the conformation), is combined with Eq. (2) to give

$$\log M = -b^{-1}\log\left(\frac{w^2}{6V^0A}\right) + b^{-1}\log\frac{t_r}{t^0V_c} \qquad (5)$$

This allows the molar mass values obtained under differing flow conditions to be more readily compared, since they can be plotted graphically along a common normalised abscissa, the values of which being proportional to the reciprocal diffusion coefficient (cf. Eq. (2)). Such plots are shown in Fig. 5 for the different flow-rate conditions used in Fig. 4. The slope of these plots (dlog M/dlog t_r), which should only depend on the conformation of the polymer, should be constant if no conformational changes in the distribution appear. The linear centre part of curve B ($V_c=0.75$ ml/min) covers a broader range of molar masses than the centre-part of curve A does, although it has approximately the same slope (1.48 as compared with 1.52 for curve A). The conformational parameter b (Eq. (5)), equal to the inverted slope, is thus around 0.7 for both curves. This can be regarded as reasonable since it indicates an expanded conformation, as was expected for this polymer. The

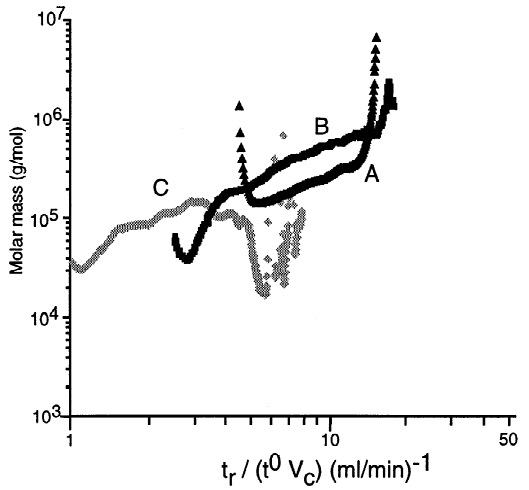

Fig. 5. Double log plot of molar mass versus the normalised retention level t_r/t^0V_c for HPMC 10000 at different flow-rates. Conditions: identical to Fig. 4.

fact that the centre-part of curve A underestimates the molar masses as compared with curve B is difficult to explain, although it should be kept in mind that the experimental conditions are the least favourable in this case. The retention level is low and there are difficulties in defining a correct baseline for the detector signals due to the disturbances in the vicinity of the void (see Fig. 3A).

The central and useful part of curve C ($V_c = 2.0$ ml/min) represents an interval in which the slope is similar to that of curve B. This provides evidence of a fractionation having occurred. Since if this interval is extrapolated to higher $t_r/(t^0 V_c)$ values, curve C coincides with curve B, it appears likely that they represent different fractions of the same sample. Evidently, it is necessary to use several different flow conditions so as to cover the entire range of a broad molar mass distribution of a polymer. The broader molar mass range covered and the much higher recovery obtained under the conditions used in the case of curve B than in that of curve C, clearly indicates the flow conditions to be better in the case of curve B. However, it should be noted that neither curve B nor C provides reliable information on molar masses below the level of 100 000 g/mol.

The cumulative molar mass distributions obtained for each of the three different conditions can be seen in Fig. 6. Curve A ($V_c = 0.25$ ml/min) is very steep, suggesting the polydispersity to be low, a result of the poor fractionation of the molar masses at these flow-rates. There is a rather limited range of the total sample for which reliable masses were obtained, as was discussed in connection with Figs. 4 and 5. Thus, over 90% of the molar masses registered for curve A appear in the narrow range of 120 000 g/mol up to 400 000 g/mol. The remaining fraction represents the very broad range of 400 000 g/mol to 10 million g/mol of molar mass. As was indicated above, this is most likely an artifact. Although, the better fractionation obtained after the increase in V_c to 0.75 ml/min (curve B) gave a broader distribution, but the observed molar masses below 100 000 g/mol may be inaccurate. The loss in information regarding the high molar mass components discussed already for curve C ($V_c = 2.0$ ml/min) in Fig. 4, is clearly illustrated here. The other two modified celluloses show a flow-rate sensitivity similar to that for HPMC 10000.

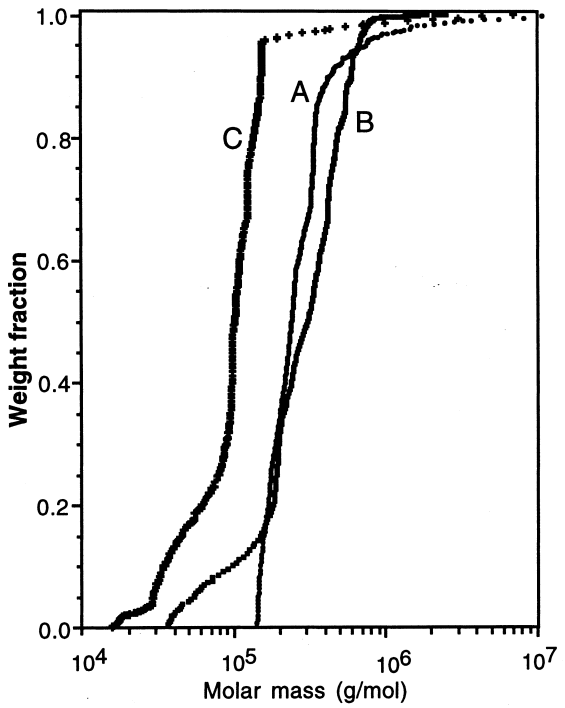

Fig. 6. Cumulative molar mass distribution for HPMC 10000 at different flow-rates. Conditions: identical to Fig. 5.

Another way of demonstrating the effects of different flow-rates is shown in Fig. 7, in which the polydispersity indices, M_w/M_n, obtained and recovery are plotted for HPMC 4000 for the various crossflow-rates employed. The results are similar to those obtained for HPMC 10000, there being a decrease in recovery at high V_c. The influence of the different crossflow conditions on the observed polydispersity index is evident. At low V_c, M_w/M_n values close to 1 are obtained. These increase, to a maximum of 2 for a V_c of 0.75 ml/min, and then decrease as V_c increases. As for HPMC 10000, too low a crossflow appears to have resulted in poor resolution and in the narrow distribution that was observed, whereas too high a crossflow led to a loss of the high molar mass components. Accordingly, the observed maximum polydispersity index appears to be the most reliable measured here.

The flow-rate studies above illustrate the difficulties encountered in obtaining a suitable retention level for all components when the distribution is broad. Accordingly, several crossflow-rates need to

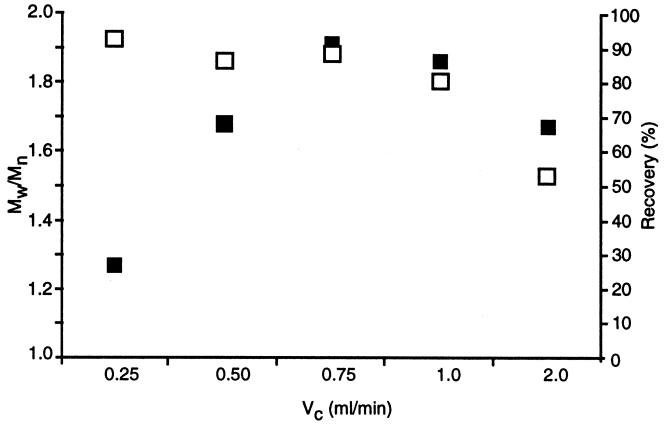

Fig. 7. Polydispersity index M_w/M_n (■) and the recovery (□) for HPMC 4000 at different crossflow-rates. The outlet flow-rate was held constant at 1 ml/min. The sample concentration was 5.14 mg/ml.

be used to cover all components. One solution may be to use a programmed field where the crossflow-rate is changed during elution, allowing more suitable retention levels for the different sizes contained in the distribution to be found more readily. The difficulty in working at high crossflow-rates is most probably an effect of the low overload concentration of these viscosity regulating polymers. Similar effects have been observed by Adolphi and Kulicke [23] for high molar mass pullulan. At a high V_c the concentration of the polymer near the accumulation wall is increased. This could easily provoke chain entanglements which could result, for example, in the sudden decrease in recovery observed for higher crossflows, as discussed in connection with Fig. 3.

4.2. Concentration effects

In working with flexible polymers, sample concentration is a fundamental experimental parameter. Concentrations being too high can lead to interactions between the chains, changing the solution behaviour of the polymers dramatically. Clear effects of high sample concentrations, so-called overloading effects, on the elution behaviour of polymers in flow FFF have been reported [22]. This appears crucial for expanded polymers since these usually have a relatively low overlap concentration and are subject to entanglement, which can affect the determination of molar mass.

The sample zone concentration in the separation channel obviously differs from that in the test tube. Normally, a dilution of the sample occurs, resulting in the concentration in each slice that the detectors encounter being considerably less than in the original test tube. This is necessary if the influence of the second virial coefficient should be neglected in the light scattering relation (Eq. (3)). Since there is an exponential concentration profile in the channel, the zone concentration near the ultrafilter is high [11], which can facilitate interactions between the polymer chains in that region. Another artifact can arise from interactions between the polymer and the ultrafilter. Accordingly, it is desirable to work at low concentrations. At the same time the MALS detector requires a relatively high sample load, at least for low molar masses. The signal-to-noise ratio can nevertheless be somewhat improved by the use of an inline filter directly after the channel [8]. However, the effects on the observed results when using such filter should be carefully examined.

These limitations force the user to work within a rather small concentration range, especially with polymers. It is therefore important, to routinely study the effects of the sample concentration in flow FFF–MALS analyses of polymers.

The three HPMC-samples examined were analysed at five different concentrations in the range of 1 mg/ml to 12 mg/ml, corresponding to an injected mass of approximately 20 μg to 240 μg. The crossflow-rate selected was 0.75 ml/min, which kept the outlet flow-rate at around 1 ml/min. Interestingly

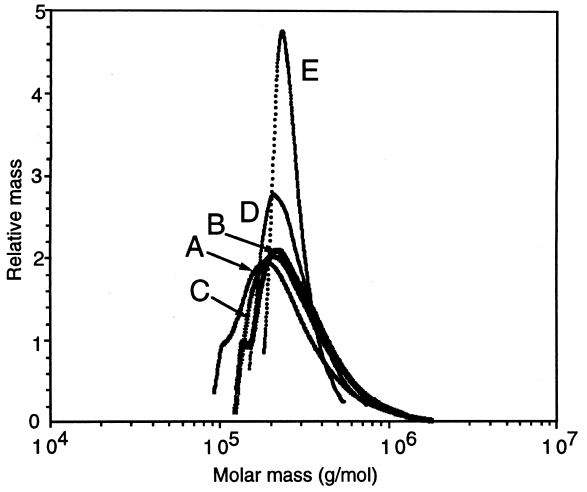

Fig. 8. Molar mass distribution for different concentrations of HPMC 10000. Note the decrease in obtained polydispersity when the concentration is increased. Concentrations: (A) 1.61 mg/ml, (B) 3.80 mg/ml, (C) 5.14 mg/ml, (D) 8.24 mg/ml and (E) 11.6 mg/ml. The flow conditions were: $V_{in}=1.75$ ml/min; $V_c=0.76$ ml/min; $V_c/V_{out}=0.77$; $t^0=0.29$ min.

enough, there were small differences in the weight average molar mass, M_w, obtained when the concentration was changed. For HPMC 10000, the observed M_w was approximately 310 000 g/mol, except for the highest mass injected, for which it was lower, 260 000 g/mol. The molar mass distributions for HPMC 10000 obtained at the different concentrations are shown in Fig. 8. Although the distributions coincide fairly well, for the two highest sample concentrations, 8 mg/ml and 12 mg/ml a tendency towards more narrow distributions is evident (curves D and E). For curve E, the polydispersity index M_w/M_n was only 1.2, compared with 2.0 for the more diluted samples, curves A to C. Also, the smallest amount injected, 20 μg, was problematic since the results were irreproducible due to the weak response of the MALS detector.

A further illustration of concentration effects was obtained by determination of the polydispersity index and of recovery for different concentrations of HPMC 4000 (Fig. 9). Concentrations below 5 mg/ml gave high recovery (>85%) and a constant polydispersity index of about 1.9. As observed for the HPMC 10000 sample as well, a drop in polydispersity was observed when the concentration was increased to 8 mg/ml and to 12 mg/ml. This was accompanied by a dramatic decrease in recovery, to less than 50% for the highest sample concentration. The concentration effects of HPMC 50 were similar, although a higher concentration (5 mg/ml) was required for obtaining an adequate MALS signal due to the molar mass being lower.

These results illustrate the difficulties that can arise when one works with high sample concentrations of flexible polymers. From the aforementioned, it is clear that too high a sample load results in an underestimation of polydispersity. This appears to be caused by a drop in resolution, due to a deterioration in size separating ability. The concomi-

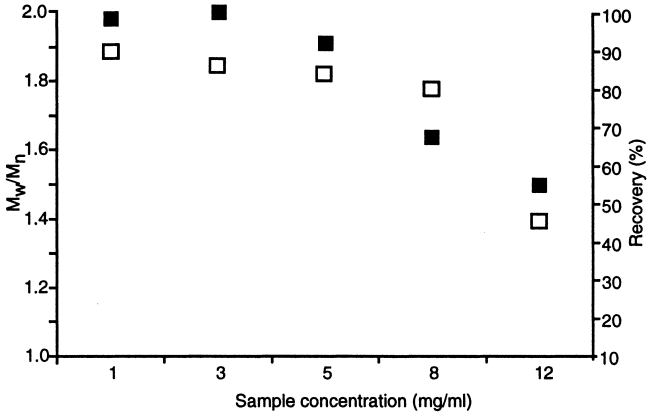

Fig. 9. Polydispersity index M_w/M_n (■) and the recovery (□) for HPMC 4000 at different concentrations. The flow-rates were $V_{in}=1.75$ ml/min; $V_c=0.76$ ml/min; $V_c/V_{out}=0.77$; $t^0=0.29$ min.

tant decrease in recovery, on the other hand, suggests there to be a connection between the decrease in these two parameters. Since the observed M_w was significantly lower at high sample concentrations, it could not be excluded that there is also a loss of high molar mass materials. Large components, since they travel relatively close to the channel wall, are present there in high concentrations and may thus have been subjected to overlapping effects. Since this leads to excessive retention levels, this sample fraction may not be detected. Consequently, sample concentration is another important parameter that needs to be studied carefully when working with flow FFF–MALS.

4.3. Molar mass and radius of gyration of HPMCs

When the optimum experimental conditions had been obtained, it was possible to focus on the characterisation of the HPMC samples. Analyses were performed at a V_c about 0.75 ml/min, the concentration being approximately 5 mg/ml for each of the three HPMC samples. The obtained molar mass and the radii of gyration under these conditions are shown in Table 1. As expected, the three samples differ in molar mass and size. In terms of the osmometry data (Table 1), the molar mass of HPMC 4000 and 10000 should be rather similar [12]. As can be seen in Table 1, HPMC 10000 had an M_w of 309 000 g/mol and an r_{Gz}, of 73 nm whereas HPMC 4000 is smaller with an M_w of 225 000 g/mol and an r_{Gz}, of 68 nm. As expected, the observed M_w of HPMC 50 was lower, about 130 000 g/mol. However, r_{Gz}, 58 nm, was only slightly less than for the other two samples. The relation between the molar mass and the radius of gyration differs considerably from that of the pullulans and dextrans studied earlier [8]. At an M_w of 95 000, for example, pullulan had an r_{Gz}, of only 12 nm. It can thus be concluded that the HPMCs are much larger in size relative to their mass, indicating a more expanded conformation. The more complex solution behaviour observed for the HPMCs thus appears related to the large r_{Gz} of these samples. Their overlap concentration must be significantly lower than that of the pullulans and dextrans. The large r_{Gz}, observed for all three HPMC samples can also explain their similarity in behaviour observed in the flow-rate and concentration studies reported above.

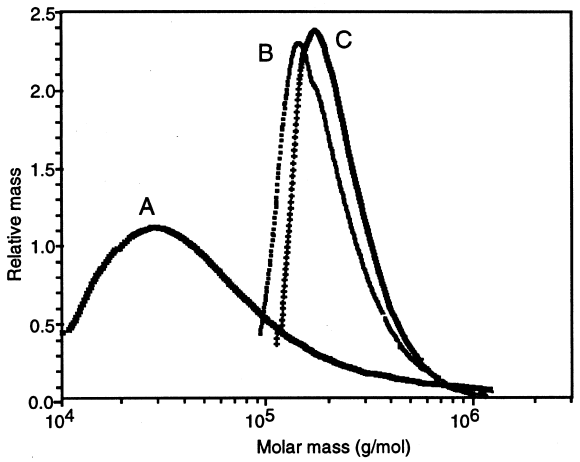

Fig. 10. Molar mass distribution for (A) HPMC 50, (B) HPMC 4000 and (C) HPMC 10000 obtained at a sample concentration of approximately 5 mg/ml. The flow-rates were: (A) $V_{in}=1.75$ ml/min; $V_c=0.80$ ml/min; $V_c/V_{out}=0.84$; $t^0=0.30$ min; (B) $V_{in}=1.75$ ml/min; $V_c=0.76$ ml/min; $V_c/V_{out}=0.77$; $t^0=0.29$ min; (C) $V_{in}=1.75$ ml/min; $V_c=0.75$ ml/min; $V_c/V_{out}=0.75$; $t^0=0.29$ min.

The molar mass distributions are shown in Fig. 10. The distributions of HPMC 10000 and HPMC 4000 are rather similar. The polydispersity index for these two samples is of moderate size 1.9–2.0. Combined with the M_w data, it gives a corresponding number average molar mass, M_n, of 117 000 g/mol for HPMC 4000 and 158 000 g/mol for HPMC 10000. These values are somewhat higher than those obtained by osmometry, 100 000 g/mol and 120 000 g/mol for HPMC 4000 and HPMC 10000, respectively. Such discrepancies may be caused by an incomplete fractionation of the samples by flow FFF leading to a too low polydispersity index. Other possibilities are the loss of low molar mass components by penetration through the membrane (cut-off 10 000 g/mol of dextran) and erroneous detector signals due to the low signal-to-noise ratio at the low molar mass end. The HPMC 50 sample has a higher polydispersity index, $M_w/M_n=3.7$, corresponding to an M_n of 35 000 g/mol, which agrees well with the osmometry data of 31 000 g/mol.

The distributions of the radius of gyration are shown in Fig. 11. Again, there is a close resemblance between the high molar mass samples. HPMC 50 has

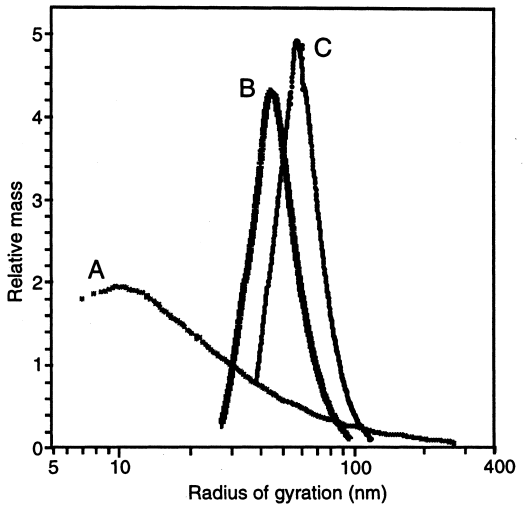

Fig. 11. Radius of gyration distribution for (A) HPMC 50, (B) HPMC 4000 and (C) HPMC 10000 obtained at a sample concentration of approximately 5 mg/ml. The flow-rates were: (A) $V_{in}=1.75$ ml/min; $V_c=0.80$ ml/min; $V_c/V_{out}=0.84$; $t^0=0.30$ min; (B) $V_{in}=1.75$ ml/min; $V_c=0.76$ ml/min; $V_c/V_{out}=0.77$; $t^0=0.29$ min; (C) $V_{in}=1.75$ ml/min; $V_c=0.75$ ml/min; $V_c/V_{out}=0.75$; $t^0=0.29$ min.

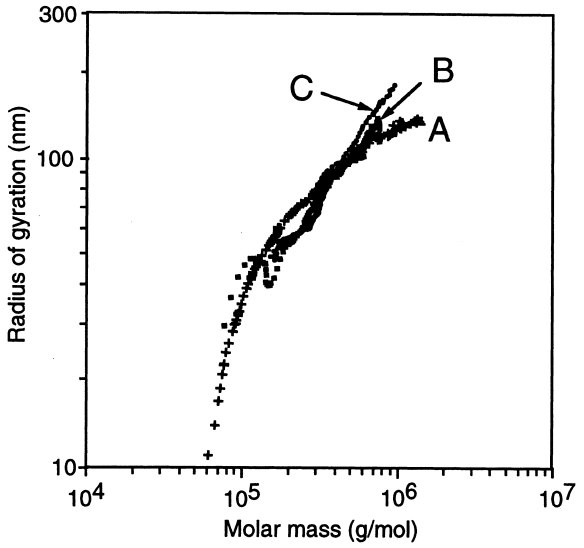

Fig. 12. Plot of the radius of gyration versus the molar mass for (A) HPMC 50 (+); (B) HPMC 4000 (■) and (C) HPMC 10000 (●). The slope γ was for (A) 0.53 (obtained in the molar mass range of 200 000 g/mol to 900 000 g/mol), (B) 0.68 (obtained in the molar mass range of 250 000 g/mol to 670 000 g/mol), and for (C) 0.71 (obtained in the molar mass range of 240 000 g/mol to 940 000 g/mol).

a wider distribution, ranging from a few nm to over 100 nm. It was not possible to obtain the complete distribution of HPMC 50 since radii below approximately 10 nm are not available for MALS [6]. The relatively high *z*-average of the radius of gyration, 58 nm, relative to its M_n and M_w, can be seen as reasonable in light of the broad distribution of the radii. The broad distributions of both the molar masses and the radii of gyration observed for HPMC 50 appear to be caused by the presence of aggregates in this sample. This can explain the observed differences in polydispersity to HPMC 4000 and HPMC 10000.

One advantage of the flow FFF–MALS combination is that it provides information on both molar mass and size distributions simultaneously making it possible to construct double log plots of molar mass versus radius of gyration [6–8]. The obtained value of the slope γ based on these plots can be used to deduce information regarding the conformation. For this information to be relevant good molar mass and size fractionations of the sample are required. These plots can thus serve as a test of the resolution obtained in the separation being satisfactory. The conformation plots for the three HPMCs are shown in Fig. 12. The slope γ is approximately 0.7 for both HPMC 4000 and 10000, which could be interpreted as random coil conformation in a good solvent. This γ-value is significantly higher than those obtained for pullulans and dextrans [8], indicating again the HPMC samples to have a more expanded structure. The γ-value obtained for the distribution of HPMC 50 is close to 0.5, indicating a more compact conformation. However, as is evident in Fig. 12, the slope decreases at high molar mass. This may indicate a shift in conformation, possibly due to aggregation. Since there was no clear indication of aggregates for HPMC 4000 and HPMC 10000, it is possible that the three HPMC samples that were examined differ somewhat in their solution behaviour. Further studies are needed to examine different

solvents in efforts to clarify the effects of solvent quality on the observed size and molar mass of these polymers.

Acknowledgements

This study was supported by grants from the Swedish Research Council for Engineering Sciences. The development of the flow FFF system was made possible by grants from Astra Hässle AB, the Carl Trygger Foundation and the Crafoord Foundation. Dr. Robert Lundqvist, Astra Hässle AB, is acknowledged for his kind gift of the HPMC samples. Dr. Stefan Nilsson and Professor Lars-Olof Sundelöf of Uppsala University are gratefully acknowledged for their comments on the work while it was in progress.

References

[1] R.C. Rowe, J. Pharm. Pharmacol. 32 (1980) 116.
[2] S. Nilsson, L.-O. Sundelöf, B. Porsch, Carbohydr. Polym. 28 (1995) 265.
[3] K. Jumel, S.E. Harding, J.R. Mitchell, K.-M. To, I. Hayter, J.E. O'Mullane, S. Ward-Smith, Carbohydr. Polym. 29 (1996) 105.
[4] J.C. Giddings, Science 260 (1993) 1456.
[5] B. Wittgren, K.-G. Wahlund, H. Dérand, B. Wesslén, Macromolecules 29 (1996) 268.
[6] P.J. Wyatt, Anal. Chim. Acta 272 (1993) 1.
[7] D. Roessner, W.-M. Kulicke, J. Chromatogr. A 687 (1994) 249.
[8] B. Wittgren, K.-G. Wahlund, J. Chromatogr. A 760 (1997) 205.
[9] K.-G. Wahlund, J.C. Giddings, Anal. Chem. 59 (1987) 1332.
[10] A. Litzén, K.-G. Wahlund, Anal. Chem. 63 (1991) 1001.
[11] A. Litzén, Anal. Chem. 65 (1993) 461.
[12] R. Lundqvist and N. Soubbotin, J. Polym. Anal. Characterisation,, submitted for publication.
[13] J.J. Kirkland, C.H. Dilks, S.W. Rementer, Anal. Chem. 64 (1992) 1295.
[14] J.C. Giddings, M.A. Benincasa, Anal. Chem. 64 (1992) 790.
[15] B. Wittgren, K.-G. Wahlund, H. Dérand, B. Wesslén, Langmuir 12 (1996) 5999.
[16] H. Thielking, D. Roessner, W.-M. Kulicke, Anal. Chem. 67 (1995) 3229.
[17] H. Thielking, W.-M. Kulicke, Anal. Chem. 68 (1996) 1169.
[18] R. Hanselmann, M. Ehrat, H.M. Widmer, Starch 46 (1995) 345.
[19] K.D. Caldwell, Anal. Chem. 60 (1988) 959A.
[20] K.-G. Wahlund, H.S. Winegarner, K.D. Caldwell, J.C. Giddings, Anal. Chem. 58 (1986) 573.
[21] A. Litzén, J.K. Walther, H. Krischollek, K.-G. Wahlund, Anal. Biochem. 212 (1993) 469.
[22] K.D. Caldwell, S.L. Brimhall, Y. Gao, J.C. Giddings, J. Appl. Polymer Sci. 36 (1988) 703.
[23] U. Adolphi, W.M. Kulicke, Polymer 38 (1997) 1513.